Title
Obstructive nephropathy: evaluation with dynamic Gd-DTPA-enhanced MR imaging.

Journal
Radiology, 175(3)

ISSN
0033-8419

Authors
Semelka, RC
Hricak, H
Tomei, E
et al.

Publication Date
1990-06-01

DOI
10.1148/radiology.175.3.2343131

Peer reviewed

Richard C. Semelka, MD • Hedvig Hricak, MD • Ernesto Tomei, MD • Andreas Floth, MD • Marshall Stoller, MD

Obstructive Nephropathy: Evaluation with Dynamic Gd-DTPA–enhanced MR Imaging[1]

The potential of dynamic gadolinium diethylenetriaminepentaacetic acid (DTPA)-enhanced magnetic resonance (MR) imaging for the examination of obstructive nephropathy was analyzed in 27 subjects (five healthy subjects, seven patients with dilated nonobstructed kidneys, six patients with acute obstruction, and nine patients with chronic obstruction) with use of a 1.5-T magnet. Morphologic findings were compared with quantitative analysis of temporal changes in signal intensity. Dynamic postcontrast images of the normal kidney demonstrated four phases of enhancement: cortical enhancement phase, early tubular phase, ductal phase, and excretory phase. The pattern of enhancement in dilated nonobstructed kidneys was similar to that in normal kidneys. In acutely obstructed kidneys, cortical enhancement was similar to that in normal kidneys (17% increase), but medullary enhancement was higher than normal, resulting in diminished corticomedullary differentiation. The early tubular phase was prolonged (until 2.5 minutes after injection), with delayed appearance of the ductal and excretory phases. In chronically obstructed kidneys, the increase in cortical intensity was less than that in normal kidneys (13% increase). The early tubular phase was prolonged, and the ductal phase was diminished or absent.

Index terms: Gadolinium • Hydronephrosis, 81.84 • Kidney, function • Kidney, MR studies, 81.1214 • Kidney, stenosis or obstruction, 81.84 • Magnetic resonance (MR), contrast media

Radiology 1990; 175:797–803

THE distinction between obstructive and nonobstructive hydronephrosis is an occasionally difficult but not uncommon diagnostic problem in urologic practice. The radiologic studies used in evaluating hydronephrosis are ultrasound (US), intravenous urography (IVU), computed tomography (CT), and nuclear scintigraphy. US is suitable for morphologic evaluation but does not supply information about renal function. IVU allows morphologic and, with regard to glomerular filtration rate, functional evaluation of the kidney. Sometimes, however, it may be difficult to distinguish between obstructive and nonobstructive hydronephrosis on the basis of IVU findings. Dynamic contrast material–enhanced CT is a tomographic technique with excellent spatial and temporal resolution (1), but, to our knowledge, there are no reports in the literature discussing the CT temporal changes in the evaluation of renal obstruction. CT can, however, be used to identify the level of obstruction in the presence of obstructive hydronephrosis. To date, diuretic iodine-131 iodohippurate sodium (Hippuran; Mallinckrodt, St Louis) studies have provided the most reliable data for differentiating obstructive from nonobstructive hydronephrosis (2–5). There are, however, limitations to this modality, since nonvisualization of the kidney following I-131 iodohippurate injection does not exclude obstruction, even in the presence of recoverable renal function (6). In addition, studies with I-131 iodohippurate lack spatial resolution, limiting morphologic evaluation.

Gadolinium diethylenetriaminepentaacetic acid (DTPA)–enhanced magnetic resonance (MR) imaging is presently being evaluated for its potential in the evaluation of renal function (7–11). This technique is well suited for studying the kidney, offering both excellent spatial resolution and direct multiplanar imaging capability. With use of gradient recalled acquisition in a steady state (GRASS), images can be rapidly acquired during a breath hold, providing the temporal resolution necessary to study renal parenchymal enhancement. Changes in the signal intensity (SI) of renal parenchyma are based on the concentration of the contrast agent and permit evaluation of tubular concentrating ability (7). The purpose of this study was to define the usefulness of Gd-DTPA–enhanced MR imaging in differentiating obstructive from nonobstructive hydronephrosis and acute from chronic obstruction.

SUBJECTS AND METHODS

Subjects

A total of 27 subjects were examined. There were 17 men and 10 women, ranging in age from 18 to 75 years (mean, 42 years). The study group included five healthy volunteers (10 normal kidneys), six patients with acute obstruction (six normal kidneys and six acutely obstructed kidneys), nine patients with chronic obstruction (nine normal kidneys and nine chronically obstructed kidneys), and seven patients with dilated nonobstructed kidneys (one normal kidney, 12 dilated nonobstructed kidneys, and one chronically obstructed kidney). At the beginning of the study, two of the 27 patients were examined twice. For the first study, fluid was withheld for 5 hours be-

[1] From the Departments of Radiology (Box 0628) (R.C.S., H.H., E.T.) and Urology (H.H., A.F., M.S.), University of California, San Francisco, San Francisco, CA 94143. Received September 22, 1989; revision requested November 1; final revision received January 26, 1990; accepted February 26. **Address reprint requests to** H.H.

Abbreviations: DTPA = diethylenetriaminepentaacetic acid, GRASS = gradient recalled acquisition in a steady state, IVU = intravenous urography, SI = signal intensity, SD = standard deviation.

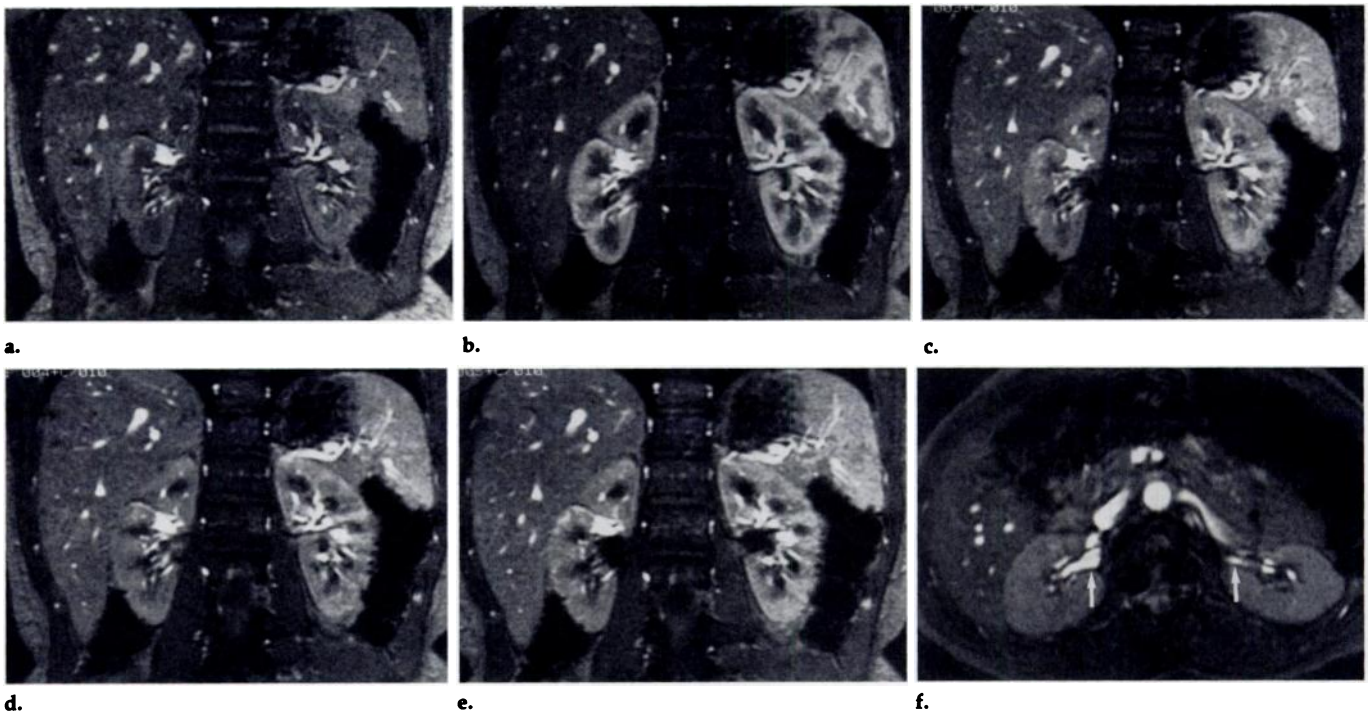

Figure 1. GRASS images of a healthy subject. **(a)** Precontrast image. Minimal corticomedullary contrast is present. **(b)** Cortical enhancement phase. Cortex SI is increased by 17%. Columns of Bertin are well visualized. Corticomedullary boundary is distinct due to differential blood flow. Note high increase in SI of spleen with serpiginous low-SI bands (normal appearance) and lower increase in SI of liver. **(c)** Early tubular phase. SI of medulla is transiently increased while there is little change in cortical SI. **(d)** Ductal phase. SI of medulla is decreased (6% from vascular phase) due to concentration of Gd-DTPA in distal convoluted tubules and collecting ducts. There is minimal decrease in cortical SI (2%). Decreased SI is apparent in the inner medulla and therefore mainly represents concentrated Gd-DTPA in collecting ducts. **(e)** Excretory phase. Concentrated (low-SI) urine appears in renal collecting systems. **(f)** Excretory phase (15 minutes after injection). No corticomedullary contrast is apparent. Urine contains dilute (high-SI) Gd-DTPA (arrows) because of rapid clearance of Gd-DTPA from the body.

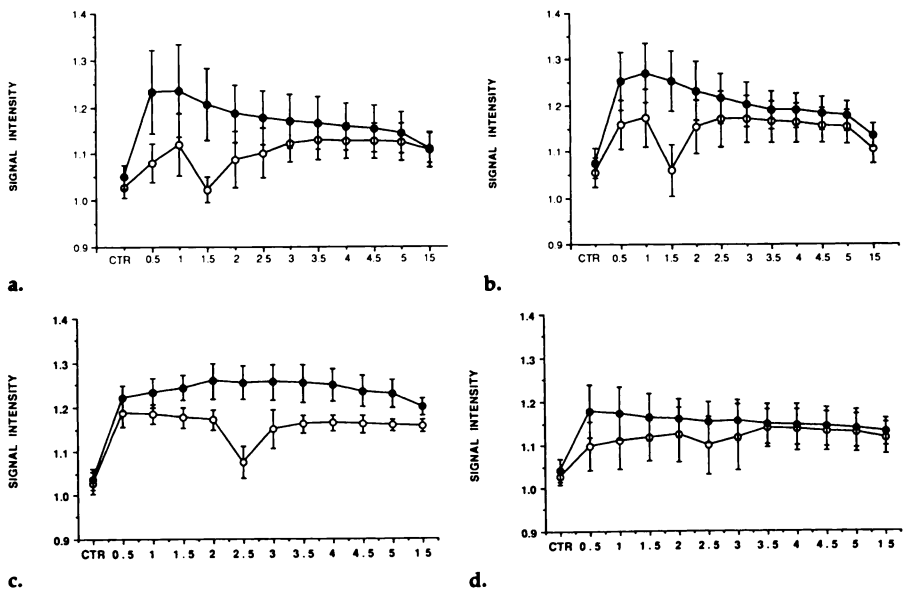

Figure 2. Temporal course of SI changes for renal cortex (O) and medulla (●). SI is expressed as a ratio to SI of psoas muscle. Bars represent standard deviation (SD). Horizontal axis shows time, expressed in minutes; *CTR* = control (preinjection). Kidneys grouped into each classification included all kidneys of that type from the entire study population. For normal and dilated nonobstructed kidneys, only those kidneys in which the early tubular phase was well demonstrated were included in the calculations. **(a)** Normal kidneys (n = 14). **(b)** Dilated nonobstructed kidneys (n = 8). **(c)** Kidneys with acute renal obstruction (n = 6). **(d)** Kidneys with chronic renal obstruction (n = 10).

fore imaging. For the second study, the patients were well hydrated by means of oral or intravenous administration of approximately 200 mL of fluid 30 minutes before imaging. All other subjects were examined after 5 hours of fluid and food restriction. Informed consent was obtained from all patients in accordance with requirements of the Institutional Review Board for Protection of Human Subjects.

MR findings were compared with the findings from clinical and appropriate radiologic studies (IVU in 19 cases, percutaneous nephrostography in four cases). Acute obstruction was defined as the onset of obstruction, as evidenced by the history and/or radiologic findings, within 3 days (12). All cases were high-grade obstruction as demonstrated at IVU and were due to renal calculus. IVU inclusion criteria were delayed appearance of contrast material in the collecting system until 10–15 minutes after the injection, increasing nephrogram, and demonstration of little or no passage of contrast material beyond the obstructing calculus.

Chronic obstruction was defined as obstruction of longer than 3 months duration (12). All cases were high-grade or complete obstruction. Inclusion criteria included delayed appearance of contrast material in the collecting system until 10–15 minutes after the injection and demonstration of little or no passage of contrast material beyond the level of obstruction. The causes of chronic obstruction included renal calculus (n = 6), surgical complication after calculus removal (n = 1), malignant retroperitoneal fibrosis (n = 1), and ureteropelvic junction fibrosis (n = 1).

The causes of dilation of nonobstructed kidneys included calculus removal (n = 1), long-standing bladder outlet obstruction due to prostatic hypertrophy relieved by Foley catheter drainage (n = 1), bladder cancer with percutaneous renal drainage (n = 1), cervical cancer with percutaneous renal drainage (n = 2), retroperitoneal benign fibrosis with unilateral drainage and contralateral obstruction (n = 1), and bilateral repaired ureteropelvic junction obstruction (n = 1). In all cases of dilated nonobstructed kidneys, obstruction had been relieved for a minimum of 3 days.

Absence of obstruction was confirmed with percutaneous nephrostography in four cases and with IVU in three cases. Inclusion criteria included visualization of free drainage of contrast material from the renal collecting system through the percutaneous nephrostomy tube at percutaneous nephrostography or a normal-appearing nephrogram and normal temporal appearance of contrast material in the collecting systems at IVU. The Whitaker test was not performed in any of the subjects.

Imaging Technique

MR images were obtained on a 1.5-T cryogenic magnet (Signa; GE Medical Systems, Milwaukee). GRASS images (repetition time = 33 msec, echo time = 13 msec, flip angle = 70°) were obtained at one or two levels in the axial or coronal plane with flow compensation. The field of view was 32–38 cm^2. The matrix size was 256 × 128, and two excitations were used. A bolus injection of gadopentetate dimeglumine (Magnevist; Berlex Imaging, Wayne, NJ) Gd-DTPA (0.1 mmol/kg of body weight) was followed immediately by acquisition of GRASS images (the first at 0.5 minute and subsequent ones every 0.5 minute for 5 minutes). At 15 minutes after the injection, a repeat GRASS image was obtained. There were no changes in any imaging parameters between the GRASS image acquisitions. Image acquisition took 13 seconds per image and was performed during a breath hold in all subjects.

Image Analysis

The data were analyzed both qualitatively and quantitatively. Qualitative analysis was performed by means of visual assessment by two of the authors (R.C.S., H.H.). Changes in SI, the time course of enhancement, the pattern of enhancement (uniform or patchy), and the morphologic appearance of the kidney (renal size, cortical and medullary thickness, and size of the collecting system) were evaluated.

Quantitative analysis was performed by one of the authors (E.T.), who was blinded to the diagnosis, on a remote console with regions of interest placed manually over the renal cortex, renal medulla, renal calyces, liver, spleen, retroperitoneal fat, and psoas muscles. The size of the region of interest was 0.08 cm^2. Region-of-interest measurements were made bilaterally in the cortex, medulla, and collecting system of the upper, middle, and lower portions of the kidneys. Four determinations were made in the liver, spleen, perirenal fat, and psoas muscles of each subject. A total of 11,016 data points were processed. Because SI varies from image to image and from side to side, it was expressed as the ratio of the SI of the tissue of interest to the SI of the ipsilateral psoas muscle on the same image. In addition, renal cortical to medullary contrast was expressed as the SI of the cortex minus the SI of the medulla, divided by the SI of the psoas muscle. The percentage of contrast was calculated as the absolute value of two measurements divided by the mean of the two measurements. The percentage of SI increase was calculated as the difference between two measurements divided by the first of the two measurements. All calculations were made on mean values.

RESULTS

Images were of diagnostic quality in all cases, and no subjects were excluded from the study. None of the subjects experienced any adverse effects after the Gd-DTPA injection.

Normal Kidneys

In normal kidneys, the precontrast GRASS image demonstrated minimal corticomedullary differentiation (2.3% difference) (Fig 1). After injection of Gd-DTPA, the pattern of enhancement demonstrated four phases: cortical enhancement, early tubular, ductal, and excretory.

In the cortical enhancement phase, seen at 0.5 minute after Gd-DTPA injection, both the cortex and the medulla demonstrated signal enhancement. The SI increase in the cortex, including the columns of Bertin, was 17%. The SI increase in the medulla was 5%. The disparity in corticomedullary enhancement (13% contrast) allowed excellent differentiation (Fig 1b).

In the early tubular phase, apparent at 1 minute after injection, the SI of the cortex remained similar to that in the cortical enhancement phase, but there was increased enhancement of the medulla, decreasing corticomedullary differentiation (12.6% contrast) (Fig 1c). In 12 of 26 normal kidneys, this phase was too brief to be isolated with a temporal resolution of 30 seconds between images.

In the ductal phase, which appeared at 1.5 minutes after injection, there was a slight decrease in the SI of the cortex (2%), with decreased appreciability of the columns of Bertin. The SI of the medulla, however, decreased to a greater extent (6% from the cortical enhancement phase, and 1% from precontrast levels), once again accentuating corticomedullary differentiation (20% contrast) (Fig 1d).

In the excretory phase, which appeared at 2 minutes after injection, the SI of the cortex decreased, whereas the SI of the medulla increased (except for the papillary region, which appeared even darker), resulting in loss of the corticomedullary boundary. The calyces and infundibula were demonstrated for the first time during this phase, showing the low SI of concentrated Gd-DTPA in the urine (Fig 1e). In three patients, pronounced susceptibility-induced image distortion of the collecting systems was present. In the 15-minute GRASS image, the excreted urine became higher in SI (Fig 1f).

Figure 2a demonstrates the temporal course of SI changes in the cortex and medulla. For normal kidneys, renal size ranged from 10 to 13 cm (mean, 12 cm), the cortex measured 0.5–1.0 cm in thickness (lateral to the renal hilum) with distinct columns of Bertin, and the medulla was conical.

Dilated Nonobstructed Kidneys

Dilated nonobstructed kidneys demonstrated the normal pattern of the four phases of enhancement (Fig 2b). Images demonstrating the ductal and excretory phases are shown in Figure 3. In two patients, pronounced susceptibility-induced image distortion of the renal collecting systems was seen during the excretory phase. The kidneys tended to be larger than normal, measuring 10–15 cm (mean, 13.5 cm). The cortex was of normal thickness, but the renal medulla appeared flattened.

Acute Obstruction

In acute obstruction, the appearance of the cortical enhancement phase was similar to that in normal kidneys but with a higher SI increase in the medulla (15.5% vs 5.0%, resulting in diminished corticomedullary contrast [2.8%]). The early tubular phase was prolonged, and cortical and medullary enhancement persisted until 2.5 minutes. Concentration of Gd-DTPA in the ductal phase was delayed, appearing at 2.5 minutes, and the SI of the medulla did not decrease to the same extent as in nor-

mal kidneys. The SI of the medulla remained higher than in precontrast studies. Figure 2c illustrates the temporal SI changes in the cortex and medulla. The excretory phase was delayed until 2.5–3.0 minutes. The urine in the collecting system was of normal low SI in two patients (duration of obstruction, less than 12 hours) and of high SI in four patients (duration of obstruction, 1–3 days). In two subjects, pronounced susceptibility-induced image distortion was seen in the renal collecting system of the contralateral normal kidney. Morphologically, the kidneys were enlarged, measuring 13–16 cm (mean, 15 cm). The cortex was well preserved, but the columns of Bertin were thinned, and the medulla was flattened. The renal collecting system was dilated. Images from the cortical enhancement, ductal, and early and late excretory phases in acute obstruction are shown in Figure 4.

Chronic Obstruction

In chronic obstruction, the cortical enhancement phase demonstrated diminished parenchymal enhancement compared with that in normal kidneys (13% cortical enhancement), resulting in decreased appreciability of corticomedullary differentiation (7.1% contrast). The early tubular phase was prolonged until 2.5 minutes after injection, and the ductal phase was diminished or absent. The excretion phase was delayed or inapparent, and the urine in the collecting system was of high SI. In two of these subjects, the contralateral normal kidneys showed pronounced susceptibility-induced image distortion during the excretory phase. Selected postcontrast images are shown in Figure 5. Figure 2d illustrates the temporal SI changes in the cortex and medulla. The renal length ranged from 13 to 15 cm in six of the nine patients and from 7.5 to 10 cm in three patients. The cortex was normal in four of the nine patients but thinned in five, and the columns of Bertin were always compressed and occasionally (in two patients) not perceived. The medulla was invariably compressed. In three of the patients with cortical thinning, the cortical enhancement was patchy, and the temporal changes in the medulla were heterogeneous.

Both bilateral and unilateral obstructions were present in this group. Although in unilateral obstruction the contralateral kidney functions differently from normal due to the increased blood flow and glomerular filtration (12), the pattern of enhancement was not different from that in the kidneys in healthy subjects; therefore, the contralateral kidneys were included with the kidneys from healthy subjects in the quantitative analysis.

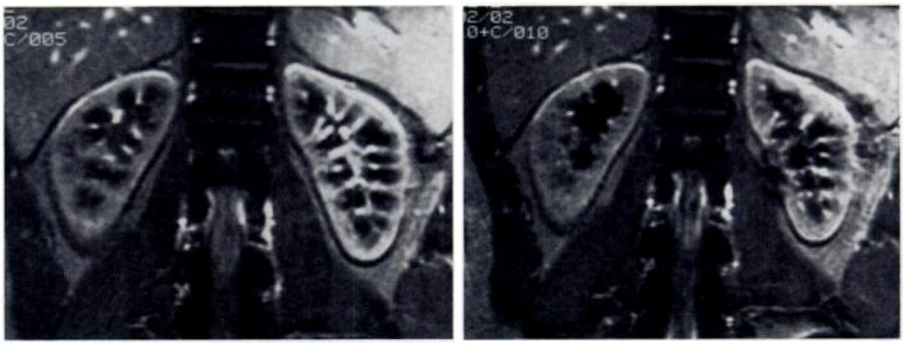

a. b.

Figure 3. GRASS images of a subject with a dilated nonobstructed kidney on the right and a normal kidney on the left. **(a)** Ductal phase. Low SI of medulla appears simultaneously in the dilated nonobstructed right kidney and in the normal left kidney. **(b)** Excretory phase. Excretion of concentrated urine appears symmetrical bilaterally. Note susceptibility-induced image distortion of the renal collecting systems due to the high concentration of Gd-DTPA.

Spleen, Liver, and Psoas Muscle

The enhancement patterns of the spleen and liver were also determined. The temporal course is illustrated in Figure 6. Values for the spleen are the mean for all subjects in the study. The spleen showed a marked initial SI increase, with a heterogeneous appearance in 12 subjects (Fig 1b). At 1 minute, the SI became homogeneous in all subjects, and there was a slow decline in enhancement. Analysis of SI enhancement of the liver revealed two patterns. In patients with a history of chronic renal obstruction, the liver enhancement was increased and prolonged compared with that in healthy subjects, patients with dilated nonobstructed kidneys, and patients with acute renal obstruction. The psoas muscles demonstrated an SI increase of 3.0% ± 1.7% (mean ± SD) on the initial postcontrast image.

DISCUSSION

The use of MR contrast media in renal imaging has been described in animal models (the rabbit [7,8] and the Yucatan micropig [9,10]) and in humans (11). Early studies demonstrated the usefulness of MR contrast media in the assessment of renal function and its potential in the diagnosis of obstruction (11). This study confirms previous results and further extends the findings.

Technique

Breath-hold GRASS technique was used to allow dynamic assessment of contrast enhancement. SI measurements were performed to quantify the degree of enhancement and to demonstrate its temporal course. Since a number of variables (eg, field strength, gradient strength, band width, radio frequency, receiver attenuation, echo time, repetition time, flip angle, magnetic susceptibility of the subject) contribute to the relative SI of tissues, and since absolute, and even relative, SIs may not be comparable between different experimental designs, the data were expressed as the ratio of the SI in the tissue of interest to the SI in the ipsilateral psoas muscle. The psoas muscle was selected because, although there is minimal psoas enhancement with Gd-DTPA administration (an average of 3% increase in SI), the muscle was uniformly identified and homogeneous, unlike perirenal fat, which on occasion was heterogeneous and sometimes too scant to quantify. By expressing the data as ratios, side-to-side variation due to magnetic-field inhomogeneity, time-related change, and magnetic susceptibility differences between individuals were minimized.

The contrast agent used in this study was Gd-DTPA (gadopentetate dimeglumine), which is freely filtered at the glomerulus and is neither secreted nor reabsorbed by the tubules (13). We hypothesize that the cortical enhancement phase is mainly due to the presence of contrast material in the intravascular and interstitial spaces and to a smaller degree in the proximal convoluted tubules. The early tubular phase is due to the presence of Gd-DTPA predominantly in

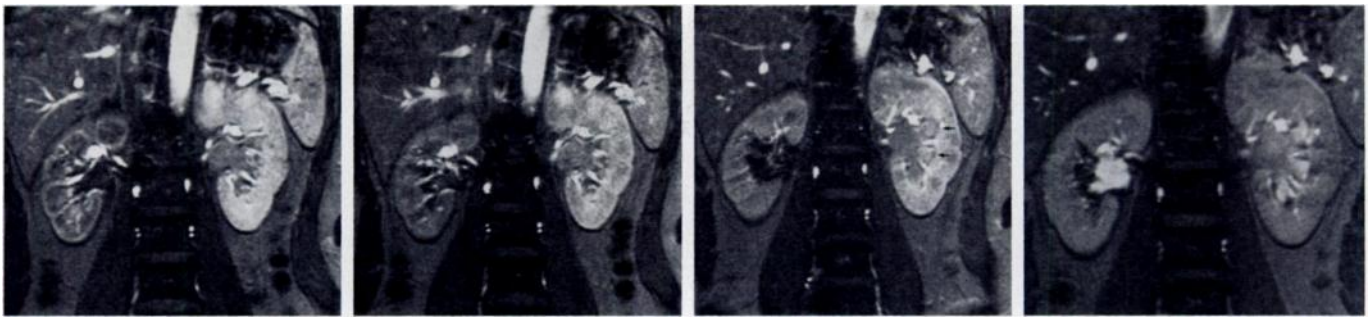

a. b. c. d.

Figure 4. GRASS images of a subject with an acutely obstructed kidney on the left and a normal kidney on the right **(a)** Cortical enhancement phase. Acutely obstructed left kidney is larger and swollen compared with the right kidney. Obstruction to venous drainage results in abnormal pattern of contrast enhancement on obstructed side, with increased parenchymal SI and decreased corticomedullary distinction. **(b)** Ductal phase. Tubular concentration is apparent on normal right side but not on the obstructed left side. Cortical enhancement is persistent on the obstructed side analogous to the persistent nephrogram on IVU examinations. **(c)** Excretory phase. Delayed image obtained at 3.5 minutes shows dilute (high-SI) urine in dilated calyces on the left (arrows). Concentrated (low-SI) urine is excreted from the right kidney. **(d)** Excretory phase (15 minutes after injection). Dilute urine is excreted on the normal side. Excretion into dilated calyces can be better appreciated.

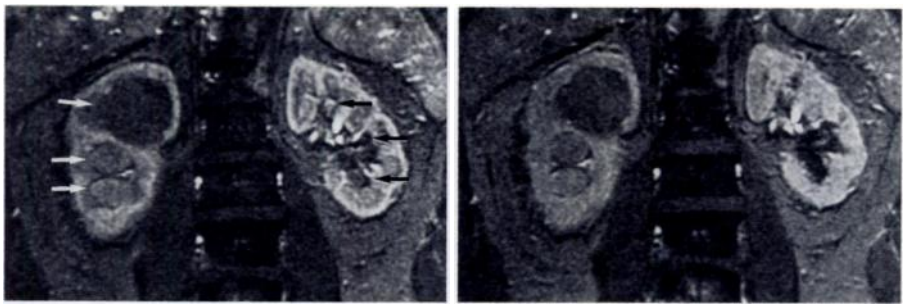

a. b.

Figure 5. GRASS images of a subject with a chronically obstructed kidney on the right and a dilated nonobstructed kidney on the left. **(a)** Cortical enhancement phase. Normal corticomedullary enhancement on the left demonstrates corticomedullary distinction. Cortical enhancement is lower in chronically obstructed kidney on the right, with no distinction between cortex and medulla apparent. Low-SI Gd-DTPA–free urine is present in both collecting systems (arrows). **(b)** Excretory phase. Concentrated urine is excreted by the dilated nonobstructed left kidney. There is no apparent excretion by the chronically obstructed right kidney, no development of corticomedullary contrast, and no significant change in parenchymal SI from the cortical enhancement phase.

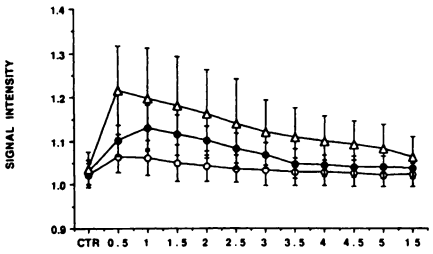

Figure 6. Temporal SI changes in the spleen (△) and liver. Liver enhancement followed two patterns: that seen in patients with a history of chronic renal obstruction and in subjects with acute obstruction in normal kidneys (●) and that seen in subjects with dilated nonobstructed kidneys (○). SI is expressed as a ratio to SI of psoas muscle. Bars represent SD. Horizontal axis shows time, expressed in minutes; *CTR* = control (preinjection).

the proximal tubules. The ductal phase reflects concentration of Gd-DTPA in the distal convoluted tubules and collecting ducts. The excretory phase reflects excretion from the collecting ducts into the calyces. The tissue SI after Gd-DTPA injection depends on its concentration (11). While this paramagnetic contrast agent always shortens both T1 and T2, at lower concentrations (0.63–6.3 mmol/L) T1 shortening predominates, resulting in tissue enhancement on T1-weighted images. At higher concentrations (25–50 mmol/L), the effect of short T1 is maximal, and T2 shortening is the dominant effect, resulting in decreased SI of tissue on T1-weighted images (11).

The state of hydration affects the concentrating ability of the kidney, which influences the pattern of Gd-DTPA enhancement (7). In our study, hydration of the subjects was standardized so that the concentration pattern would not be influenced by total body fluid content and would mainly reflect differences in renal function. The tabulated data are from studies in which fluid intake was restricted for at least 5 hours prior to imaging. Data from two studies in which the subjects were well hydrated prior to imaging were not included. In those two patients, the four phases of enhancement could not be observed, and specifically the ductal phase (Fig 7) was not demonstrated. To definitively demonstrate the effect of hydration on the SI changes in the renal parenchyma, a larger number of patients in varying states of hydration would have to be studied. The appearance of four phases depends on the temporal resolution of the technique used, as well as on individual variations in renal transit time. The effect of hydration on renal concentrating ability has been recognized in dynamic CT as well (1).

Cortical Enhancement Phase

The cortical enhancement phase is seen at 0.5 minute after injection of Gd-DTPA. In acute obstruction, this phase is similar to that in normal subjects except that there is a higher SI increase in the medulla. The pathophysiologic basis for this may be increased medullary blood flow and congestion caused by elevated ductal and tubular pressure in acute obstruction (14,15). In chronic obstruction, however, there was greatly diminished or no corticomedullary differentiation in four of nine subjects. This probably stems from generalized vasoconstriction (12,16), which eliminates the differential blood flow.

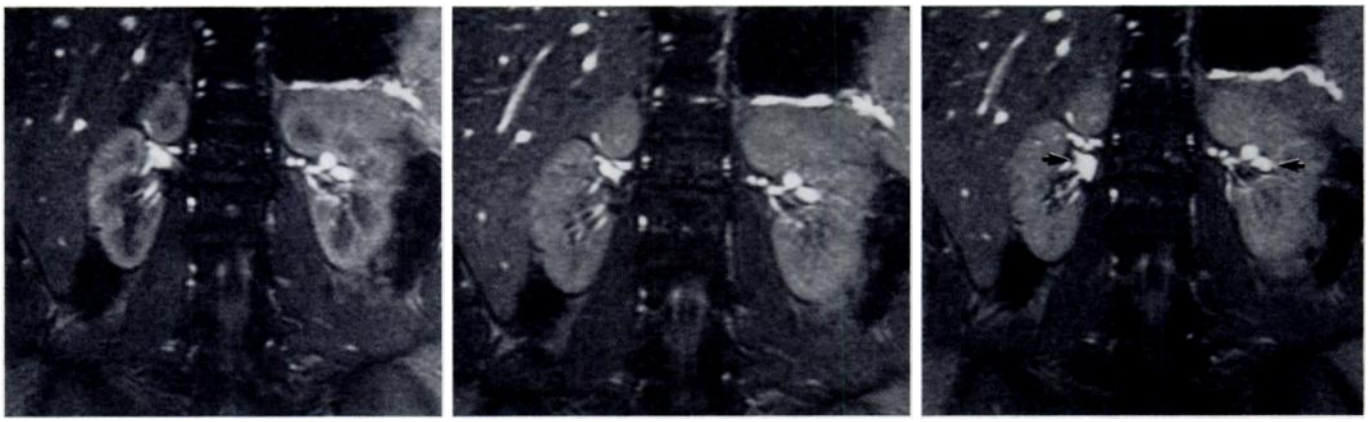

a. b. c.

Figure 7. GRASS images of healthy subject in Figure 1 while in a well-hydrated state (200 mL of fluid was administered 30 minutes before imaging). **(a)** Cortical enhancement phase. Appearance is similar to that in this phase when patient was dehydrated. **(b)** Ductal phase. Concentration of Gd-DTPA has not developed in the ductal phase because dilute Gd-DTPA is present in the distal convoluted tubules and collecting ducts, resulting in higher SI of the medulla. **(c)** Excretory phase. At 2 minutes after injection, dilute (high-SI) urine is excreted bilaterally (arrows point to renal collecting systems).

Early Tubular Phase

The early tubular phase starts at 1 minute and lasts, in normal and dilated nonobstructed kidneys, until 1.5 minutes. In acute obstruction, the early tubular phase is prolonged until 2.5 minutes, and there is persistence and a slight increase in cortical enhancement. This finding is analogous to the persistent nephrogram seen at IVU and at iodine contrast material–enhanced CT. The prolonged early tubular phase is presumably due to delay in the passage of Gd-DTPA through the tubules. The pathophysiologic basis, although controversial, is probably a combination of obstruction to venous drainage, continued filtration of contrast material into dilated collecting tubules subjected to increased pressure with continued reabsorption of water, and vasoconstriction (12,13–15,17–22). In chronic obstruction, cortical enhancement is reduced and prolonged compared with that occurring in healthy subjects. The basis for this finding is that obstruction to venous drainage causes relative ischemia, which, with time, reduces blood flow, resulting in decreased cortical enhancement (12,14,16–19,22).

Ductal Phase

In normal and dilated nonobstructed kidneys, the ductal phase appears at 1.5 minutes. In acute obstruction it is delayed, appearing at 2.5 minutes. In chronic obstruction it is delayed to 2.5 minutes or is absent. The appearance of either increased or decreased medullary SI in the ductal phase is affected by the level of antidiuretic hormone. When these levels are low (as in overhydration), water reabsorption from the collecting ducts is diminished, and free water clearance is high; as a result, the Gd-DTPA in the urine is dilute (high SI). When antidiuretic hormone levels are normal or elevated (as they are during fluid restriction), the transit time is prolonged; as a result, the Gd-DTPA in the urine is concentrated (low SI). As in the early tubular phase, the temporal resolution of imaging in this study did not allow separation of the delivery of Gd-DTPA to the distal convoluted tubules (which could be called the late tubular phase) from the delivery of Gd-DTPA to the collecting ducts (true ductal phase). In all patients with acute obstruction, there was delayed appearance of the ductal phase, which probably resulted from increased intratubular pressure and dilation of the collecting system (12,14,15). In four of nine subjects with chronic obstruction, the ductal phase was apparent at 2.5 minutes, presumably on the same basis as in acute obstruction. In the other five, concentration of Gd-DTPA in the ductal phase did not occur, possibly because of loss of tubular function due to tubular damage (20). Tubular damage, however, is not limited to chronic obstruction and can be seen in a number of renal diseases and in renal vein thrombosis.

Excretory Phase

The change in SI in the renal collecting system provides additional information. In the nonobstructed kidneys, the SI of the calyces and the infundibula was low at 2 minutes, even when the collecting system was dilated. On the delayed 15-minute image, SI in the calyces was increased, due to the dilution of Gd-DTPA. In acute obstruction, concentrated Gd-DTPA was excreted in two patients with obstruction of less than 12 hours duration. In four patients with renal obstruction of 1–3 days duration, excreted urine was dilute. In both cases, excretion was delayed until 2.5–3.0 minutes. In chronic obstruction, the renal calyces showed either increased SI or no apparent change. Lack of apparent change in SI intensity was interpreted as representing minimal or no excretion of contrast media.

SI changes were measured in the calyces rather than the renal pelvis because Gd-DTPA layers in a gradient of concentration when located in a larger structure, such as the bladder or dilated renal pelvis. SI changes in the calyces were interpreted as representing the true concentration of the urine as excreted by the renal papillae.

Since both Gd-DTPA–free urine in a dilated renal collecting system and concentrated Gd-DTPA in urine are low in SI, the distinction between the two can be a problem. At least four features can be used to distinguish them: (*a*) The low SI of Gd-DTPA–free urine is visible during the cortical enhancement phase. (*b*) The low SI of concentrated Gd-DTPA in urine is apparent only in the excretory phase after the development of low SI in the medulla during the ductal phase. (*c*) The initial part of the excretory phase is always accompanied by low SI in the papillary tips. (*d*) Susceptibility-induced distortion of the renal collecting system can ac-

company concentration of Gd-DTPA in urine (seen in 14 kidneys in this study) but does not occur with Gd-DTPA-free urine in the collecting system (10).

Spleen and Liver

The spleen showed high SI increase at 0.5 minute after injection with a heterogeneous pattern of splenic opacification in 12 of the subjects in this study. This appearance has been described in the CT literature and appears to be due to differing blood flow patterns within the various stromal compartments of the spleen (23). This was followed by a slow decrease in splenic SI.

The hepatic SI increase was more variable. Compared with subjects with normal renal function, patients with chronic renal obstruction demonstrated increased and prolonged enhancement of the SI of the liver (Fig 6). It is our hypothesis that this may be caused by vicarious excretion of Gd-DTPA (24). It has been reported, however, that glomerular filtration remains the predominant route of elimination of Gd-DTPA in patients with renal failure (25). It has been shown that there is significant correlation between creatinine clearance and total body clearance of Gd-DTPA, with the half-life of plasma Gd-DTPA ranging from 1.4 to 10 hours, depending on the severity of renal failure (25). Although some contribution from prolonged Gd-DTPA clearance was most probably present in our study as well, we hypothesize that vicarious excretion was also responsible for the increase in hepatic SI because no difference in splenic SI between the two groups was observed. In our study, however, neither delayed (24-hour) imaging nor laboratory work was performed to confirm this hypothesis. Further work on a large number of patients is required for better understanding of the pharmacokinetics of Gd-DTPA in humans.

SUMMARY

Several conclusions can be drawn from the results of this study:

1. Four phases of contrast enhancement can be recognized in the kidney, and the cortical enhancement phase can be distinguished from the ductal phase, although the two phases are similar in appearance.

2. Standardization of patient hydration may be important prior to examination.

3. In acute obstruction of less than 12 hours duration, excreted urine is concentrated. In acute obstruction of 1-3 days duration, however, excreted urine is dilute. A larger number of patients must be studied to confirm this impression.

4. Patients with chronic renal obstruction may have detectably decreased cortical enhancement.

5. Patients with chronic renal obstruction may have increased and prolonged enhancement of hepatic SI.

In summary, by evaluating both the temporal changes in renal parenchymal SI and the morphologic appearance of the kidneys, dynamic Gd-DTPA-enhanced MR imaging may permit differentiation of acute from chronic obstruction and obstructive from nonobstructive hydronephrosis. Larger numbers of patients with more varied length and severity of obstruction should be studied to determine whether this distinction can be made reliably. The morphologic detail of images acquired with dynamic Gd-DTPA-enhanced MR imaging permits appreciation of the heterogeneous function of nephrons in normal and diseased kidneys. This information may be of value when an assessment of subsegmental function of the kidneys is required. Possible clinical applications include determination of optimal percutaneous approaches to drainage and identification of the most functional segment of kidney for ureterocalyceal anastomosis. ■

References

1. Ishikawa I, Ononchi Z, Saito T, et al. Renal cortex visualization and analysis of dynamic CT curves of the kidney. J Comput Assist Tomogr 1981; 5:695-701.
2. Koff SA, Thrall JN, Keyes JW Jr. Diuretic radionuclide urography: a noninvasive method for evaluating nephro-ureteral dilatations. J Urol 1979; 122:451-454.
3. Whitfield HN, Britton KE, Hendry WF, Nimmon CC, Wiekham JE. The distinction between obstructive uropathy and nephropathy by radioisotope transit times. Br J Urol 1978; 50:433-436.
4. Britton KE, Nimmon CC, Whitfield HN, Hendry WF, Wickham JE. Obstructive nephropathy: successful evaluation with radionuclides. Lancet 1979; 1:905-907.
5. Kalika V, Bard RH, Iloreta A, et al. Prediction of renal functional recovery after relief of upper urinary tract obstruction. J Urol 1981; 126:301-305.
6. Sherman RA, Blaufox MD. Obstructive uropathy in patients with nonvisualization on renal scan. Nephron 1980; 25:882-886.
7. Choyke PL, Frank JA, Girton ME, et al. Dynamic Gd-DTPA-enhanced MR imaging of the kidney: experimental results. Radiology 1989; 170:713-720.
8. Carvlin MJ, Arger PH, Kundel HL, et al. Use of Gd-DTPA and fast gradient-echo and spin-echo MR imaging to demonstrate renal function in the rabbit. Radiology 1989; 170:705-711.
9. Tzika AA, Thurnher S, Hricak H, et al. Rapid, contrast-enhanced diuretic MR imaging of partial ureteral obstruction: experimental study in micropigs. Invest Radiol 1989; 24:37-46.
10. Thurnher S, Tzika AA, Hricak H, et al. Noncontrast and contrast enhanced MR imaging in the evaluation of partial ureteral obstruction: an experimental study in the micropig. Invest Radiol 1989; 24:544-554.
11. Kikinis R, von Schulthess GK, Jager P, et al. Normal and hydronephrotic kidney: evaluation of renal function with contrast-enhanced MR imaging. Radiology 1987; 165:837-842.
12. Wilson DR. Urinary tract obstruction. In: Schrier RW, Gottschalk CW, eds. Diseases of the kidney. 4th ed. Boston: Little, Brown, 1988; 717.
13. Barnhart JL, Kuhnert N, Douglas BA, Berk RN. Biodistribution of $GdCl_3$ and Gd-DTPA and their influence on proton magnetic relaxation in rat tissues. Magn Reson Imaging 1987; 5:221-231.
14. Suki WN, Guthrie AG, Martinez-Maldonado M, Eknoyan G. Effects of ureteral pressure elevation on renal hemodynamics and urine concentration. Am J Physiol 1971; 220:38-43.
15. Selkurt EE. Effect of ureteral blockade on renal blood flow and urinary concentrating ability. Am J Physiol 1965; 205:285-292.
16. Vaughan ED Jr, Sorenson EG, Gillenwater JY. The renal hemodynamic response to chronic unilateral complete ureteral obstruction. Invest Urol 1970; 8:78-90.
17. Heptinstall RH. Sundry conditions affecting the renal tubules. In: Heptinstall RH, ed. Pathology of the kidney. 3rd ed. Boston: Little, Brown, 1983; 1583-1585.
18. Rao NR, Heptinstall RH. Experimental hydronephrosis: a microangiographic study. Invest Urol 1968; 6:183-204.
19. Sheehan HL, Davis JC. Experimental hydronephrosis. Arch Pathol 1959; 68:185-225.
20. Schwartz MM, Venkatachalam MA, Cotran RS. Reversible inner medullary vascular obstruction in acute experimental hydronephrosis. Am J Pathol 1977; 86:425-436.
21. Solez K, Ponchak S, Buono RA, et al. Inner medullary plasma flow in the kidney with ureteral obstruction. Am J Physiol 1977; 231:1315-1321.
22. Suki WN, Eknoyan G, Rector FC Jr, Seldin DW. Pattern of nephron perfusion in acute and chronic hydronephrosis. J Clin Invest 1966; 45:122-131.
23. Glazer GM, Axel L, Goldbert HI, Moss AA. Dynamic CT of the normal spleen. AJR 1981; 137:343-346.
24. Nelson CMK, Brown RC, Culp DA. The extrarenal excretion of urographic contrast material. J Urol 1973; 110:109-110.
25. Schuhmann-Giampieri G. Pharmacokinetics of Gd-DTPA in patients with renal failure (abstr). Radiology 1989; 173(P):410.